RSC Advances

PAPER

View Article Online
View Journal | View Issue

Cite this: *RSC Adv.*, 2019, **9**, 761

Growth of hierarchical gold clusters for use in superomniphobic electrodes†

Sanghee Lee, Wuseok Kim, Changyong Yim, Kijung Yong and Sangmin Jeon *

Received 15th October 2018
Accepted 26th December 2018

DOI: 10.1039/c8ra08527g

rsc.li/rsc-advances

We developed a method to fabricate a superomniphobic gold electrode by synthesizing hierarchical gold clusters on a gold substrate and treating the surface with low surface energy materials. The reduction of gold ions was repeated several times, causing the gold microparticles to grow in random directions and form hierarchical gold clusters. Treatment of the gold structures with perfluorothiol resulted in a superhydrophobic surface that also exhibited superoleophobicity for oils and liquids with surface tensions as low as 25.6 mN. The resulting electrode was not contaminated by hydrophilic and hydrophobic liquids, and by analyzing the current–voltage characteristics of the electrode with a PEDOT:PSS solution droplet, the electrode was found to be waterproof.

Introduction

Techniques that can control and manipulate the wettability of liquids of varying surface tension have attracted much attention because of their wide range of potential applications in chemical shielding,[1] non-wetting transparent films,[2,3] oil transportation,[4,5] and membrane technologies.[6,7] It is straightforward to fabricate conventional superhydrophobic surfaces that repel high surface tension liquids like water; a low energy material coating on a surface with appropriate roughness is usually sufficient. However, more sophisticated surface designs must be fabricated to obtain a superoleophobic surface that repels low surface tension liquids like organic solvents. Although there are numerous examples of natural superhydrophobic surfaces including lotus leaves[8,9] and water strider legs,[10] there are limited examples of natural superoleophobic surfaces; one notable example is the skin of springtails.[11] Because a surface that repels lower surface tension liquids generally repels higher surface tension liquids as well, superoleophobic surfaces are also superhydrophobic with a few exceptions.[12–14] A surface exhibiting both superhydrophobic and superoleophobic characteristics is referred to as superomniphobic.

To achieve superomniphobic characteristics, a surface should possess reentrant or hierarchical textures. Various shapes of reentrant structures mimicking springtail's skins were fabricated by advanced lithography.[15–17] In the design of reentrant structures, the local texture angle should be smaller than the equilibrium contact angle. Krupenkin *et al.* fabricated reentrant silicon nanonails and honeycombs with overhang,[18] and Kim *et al.* fabricated doubly reentrant texture on silicon wafers.[19] Their work demonstrated that even without a low energy material coating, the hydrophilic silicon surface repelled almost all liquids. Although the reentrant and doubly reentrant textures are very successful in the preparation of omniphobic surfaces, their applications are limited because their fabrication requires the use of bulky and expensive clean-room-based lithography systems.

Hierarchical textures can be an efficient alternative to reentrant textures. A hierarchically structured surface reduces the solid–liquid contact area by trapping air at multiple scales; it enhances the stability of the Cassie–Baxter state which yields higher contact angles as compared to a single-scale structured surface.[20–22] Various methods including spray coating,[23,24] multiple spin coating,[25,26] and chemical etching[27,28] have been devised to fabricate hierarchical textures on different substrates like polymers,[29] glasses,[30] and metal wires.[31] However, until now, there have been very few studies on the creation of micro/nano hierarchical structures using wet-chemical methods to obtain metallic omniphobic surfaces. Also, considering that electrode contamination results in electronic device malfunction, especially in wearable sensing devices, it is important to develop a fabrication technique that creates metal electrodes with protective and omniphobic properties.

In this study, we fabricated a superomniphobic surface with hierarchical structures by using a gold reduction reaction. Using a high concentration of a reducing agent, gold ions were reduced to microparticle clusters with nanoroughness that stacked onto each other, forming hierarchical gold clusters. After perfluorination using thiolated molecules, the surface with the hierarchical gold cluster structure showed apparent contact angles higher than 150° for both water and hexadecane. Specifically, the fabricated hierarchical gold cluster surface retained a non-wetting Cassie state for liquids having a surface

Department of Chemical Engineering, Pohang University of Science and Technology (POSTECH), 77 Cheongam-Ro, Pohang, Gyeongbuk, Republic of Korea. E-mail: jeons@postech.ac.kr

† Electronic supplementary information (ESI) available. See DOI: 10.1039/c8ra08527g

tension as low as 25.6 mN m^{-1}. Finally, we patterned a desired shape of the hierarchical gold cluster structure on polydimethylsiloxane (PDMS) and applied it to the fabrication of a flexible and multifunctional electrode exhibiting ultra-water repellency.

Experimental

Materials

Gold chloride trihydrate, hydroxylamine hydrochloride isopropanol, and 3-mercaptopropyltrimethoxysilane were purchased from Sigma-Aldrich (St. Louis, MO, USA), and perfluoro octane ethyl thiol (PFT) was obtained from Fluoryx Inc. (Carson City, NV, USA). PEDOT:PSS (Clevios PH 1000) was purchased from Heraeus (Hanau, Germany). Deionized (DI) water (18.3 MΩ cm) was obtained from a reverse osmosis water system (Human Corporation, Korea).

Synthesis of hierarchical gold clusters on a silicon wafer

Hierarchical gold clusters were synthesized by a selective reduction of gold ions on a gold surface. Chrome (5 nm) and gold (30 nm) layers were sequentially deposited onto a silicon wafer using a thermal evaporator. After cleaning the sample with ethanol and DI water, a gold reducing solution comprising $HAuCl_4$ and NH_2OH in an aqueous solution was placed on the thin gold film to reduce gold ions onto the surface for 10 min. The concentration of the gold precursor solution was fixed at 18.3 mM, and the concentration of the reducing agent solution was varied from 15.7 to 192.3 mM. As shown in Scheme 1, both hierarchical gold clusters and nanoflakes were simultaneously synthesized under high NH_2OH concentration whereas only gold nanoflakes were synthesized under low NH_2OH concentration. The reduction reaction was repeated several times, and a DI water rinse was done between cycles. To make the surface hydrophobic, the substrate was immersed in a 10 mM PFT ethanol solution for 3 h at room temperature. Treating the gold surface with PFT was easy to carry out because of the high affinity between thiol and gold.

Fabrication of superomniphobic gold electrodes on PDMS

PDMS pre-polymer and a curing agent (Sylgard 184, Dow Corning) were vigorously mixed in a 10 : 1 ratio, and the solution was transferred to a small Petri dish that was kept on a flat surface for degassing (1 h in a vacuum chamber at room temperature). Then, it was cured by baking for 6 h in an oven at 80 °C, cooled, and cut into appropriately sized pieces for further study. An adhesion layer, 3-mercaptopropyltrimethoxysilane, was vapor-deposited on the pre-cut PDMS substrate, followed by the slow deposition of a 30 nm thick gold layer through a mask to achieve the desired gold pattern. Finally, the hierarchical gold cluster structure was fabricated on the PDMS–gold surface as described above for the silicon wafer.

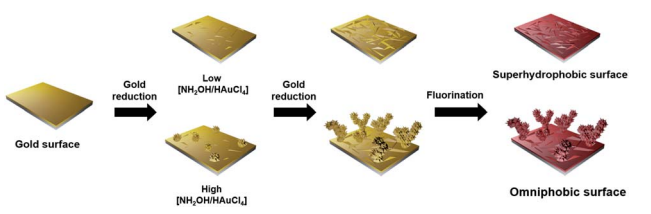

Scheme 1 Schematic illustration of the fabrication procedure for gold microparticles with superhydrophobic properties and hierarchical gold clusters with omniphobic properties.

Wetting and droplet impact analysis

The contact angle, sliding angle, and contact angle hysteresis were measured using SmartDrop (FEMTOFAB, Korea) with a 5 μL liquid droplet. Drops of fluid were released from a height of 2 cm using a 25G needle with a 1 mL syringe, and the instant motion of the bounced drop was recorded with a high-speed camera (Fastcam SA3, Photron) at a frame rate of 3600 fps.

Characterization of hierarchical gold clusters

The morphologies and crystallinity of hierarchical gold surfaces were confirmed using a scanning electron microscope (SEM, JSM-7401F, JEOL) and X-ray diffraction (XRD, D/MAX-2500, RIGAKU), respectively. Current–voltage characteristics was analysed using Keithley 2636B.

Results and discussion

The gold film deposited on the silicon wafer displayed a water contact angle of 117° after PFT treatment (Fig. 1a), indicating that it was not superhydrophobic but rather hydrophobic; since the surface did not have enough roughness to support an air interlayer between the water droplet and the surface. However, when the gold ion reduction was carried out, gold structures created enough roughness to produce superhydrophobic properties. A series of experiments were performed to investigate the influence of the $NH_2OH/HAuCl_4$ concentration ratio on the gold structures. As described in the experimental section, the concentration of $HAuCl_4$ was fixed at 18.3 mM in this study. Fig. 1b–d shows SEM images of gold nanostructures created by a reduction reaction using 15.7 mM NH_2OH; the reduction was

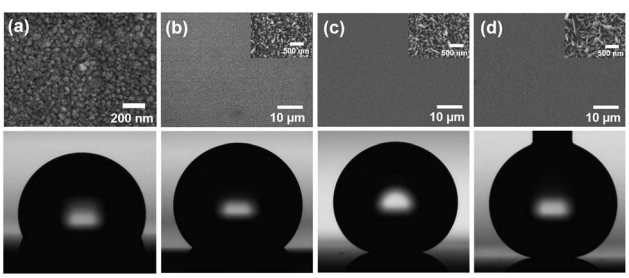

Fig. 1 (a) SEM image of gold film (upper panel) and optical microscopy image of a water droplet on the gold film after PFT treatment (lower panel). SEM images of gold nanoflake structures fabricated with (b) 1 cycle, (c) 2 cycles, and (d) 3 cycles of the reduction process (upper panel). The water contact angles on the gold nanoflake-grown surfaces after PFT treatment were 117°, 141°, 166°, and 175°, respectively (lower panel).

carried out 1 (Fig. 1b), 2 (Fig. 1c), and 3 (Fig. 1d) times, and each reduction cycle was conducted for 10 min. Since the reduction of gold ions by hydroxylamine was dramatically catalyzed on the gold surface,[32,33] the reduction reaction with a low concentration of the reducing agent induced growth on the pre-deposited gold substrate rather than nucleation of new particles in the bulk solution; therefore, a nanosized flake structure was formed selectively on the pre-deposited gold surface. When the number of reduction cycles was increased from one cycle to three cycles, the size of the nanoflakes increased and the water contact angle after PFT treatment increased to 175° as shown in the bottom panel of Fig. 1d. However, the nanoflake-grown substrates were readily wetted by liquids with low surface tension.

When the concentration of the reducing agent was high (192 mM), the reduction rate of Au^{3+} ions to the gold film increased rapidly, and hierarchical gold clusters formed simultaneously on the nanoflake surface (inset of Fig. 2a). Fig. 2 shows the morphology of the fabricated hierarchical gold clusters after repeating the reduction process several times. As the number of reduction cycles increased, the number of branches per gold cluster increased, and the hierarchical structures reached a height of 14.6 ± 4.4 μm for the 8 cycle sample. Each reduction cycle was conducted for 10 min. The gold microparticle clusters grown *via* this bottom-up synthetic process were not broken by simple washing, N_2 gas flow, and sonication. Note that the hierarchical gold clusters exhibited a highly crystalline structure with a (111) preferential orientation (see Fig. S1 in ESI†). After the resulting gold surface was chemically modified with PFT, it exhibited superomniphobic characteristics. In contrast, the surface prepared by the single reduction reaction for 60 min exhibited only superhydrophobicity (see Fig. S2 in ESI†).

Fig. 3a shows the trend in water contact angle and contact angle hysteresis as a function of the number of reduction reactions. Even when the reduction process was performed only once, the water contact angle was greater than 170°. Since the water contact angle was already sufficiently high, it did not increase significantly even when several successive reduction steps were performed. However, the contact angle hysteresis, which corresponds to the degree of adhesion between the surface and the water droplet, became smaller and was less than 1° for the 6 and 8 cycle samples. The water repellency of the hierarchical gold cluster was also verified by observing a single droplet bounce on the gold surface (Fig. 3b). When the water droplet was dropped from a height of 2 cm, it completely left the surface without wetting.

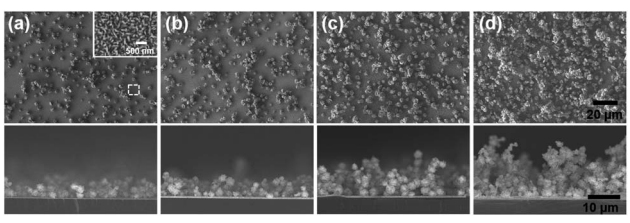

Fig. 2 Top (upper panel) and cross-sectional (lower panel) SEM images of hierarchical gold clusters fabricated by (a) 2 cycles, (b) 4 cycles, (c) 6 cycles, and (d) 8 cycles reduction cycles on the nanoflake substrate. The inset of Fig. 2a shows the magnified SEM image of the boxed region.

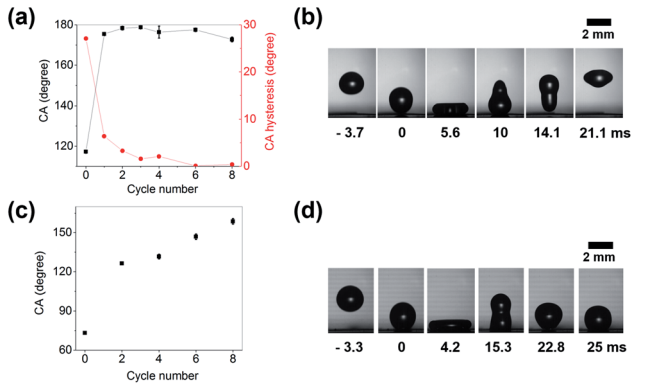

Fig. 3 Variations in (a) water contact angle (black square) and contact angle hysteresis (red circle), and (c) hexadecane contact angle as a function of the number of reduction cycles. Time-lapsed photographs of (b) water and (d) hexadecane droplets dropped from a height of 2 cm.

To demonstrate the omniphobicity of the hierarchical gold cluster, the change in the contact angle for hexadecane was measured for different numbers of reduction cycles. Fig. 3c shows that the smooth fluorinated gold surface was wet by hexadecane with a surface tension of 27.47 mN m^{-1} and exhibited a contact angle of 73.2°. However, after two cycle of reduction, the contact angle of hexadecane increased sharply to about 126.3° and then increased gradually with the number of reduction cycles, reaching 158.6° for the sample with 8 cycles. Fig. 3d shows that the hexadecane droplet released from a height of 2 cm was not fully separated from the surface after collision, because the hexadecane droplet with low surface tension wets the hierarchical gold cluster structure more than the water droplet with high surface tension (see the maximum spread diameters of a water droplet at 5.6 ms and a hexadecane droplet at 4.2 ms). Therefore, less energy was available to transform into the kinetic energy required for the droplet to bounce back completely.

A photograph of various liquid droplets, each with a different surface tension, on the hierarchical gold cluster is shown in Fig. 4a. The omniphobicity was verified based on how each liquid droplet beaded up. Fig. 4b–g shows the ability of the hierarchical gold cluster structure to maintain a range of low surface tension liquids in a non-wetting Cassie state. Starting with 1,3-propanediol that has a surface tension of 46.2 mN m^{-1}, contact angle measurements were conducted on several liquids with smaller surface tensions. Superomniphobicity was found for six low surface tension liquids, 1,3-propanediol, nitromethane, xylene, toluene, tetradecane, and dodecene; the measured contact angles (sliding angles) were 163.9 ± 1.8° (3°), 163.0 ± 1.9° (6°), 156.3 ± 0.76° (22°), 160.3 ± 1.9° (40°), 154.4 ± 3.3° (33°), and 152.4 ± 2.1° (90°), respectively. The superomniphobicity of the hierarchical gold cluster surface can be explained by the surface's unique morphology which possesses multiple scale roughness that drastically reduces the contact area between the solid and the liquid.

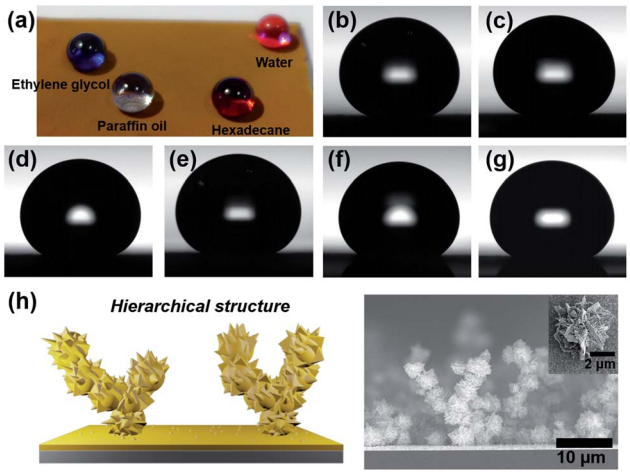

Fig. 4 (a) Photograph of the hierarchical gold cluster surface with several types of liquids. Optical microscopy images of (b) 1,3-propanediol (46.2 mN m^{-1}), (c) nitromethane (36.8 mN m^{-1}), (c) xylene (30.1 mN m^{-1}), (d) toluene (28.4 mN m^{-1}), (e) hexadecane (27.47 mN m^{-1}), (f) tetradecane (26.56 mN m^{-1}), and (g) dodecene (25.6 mN m^{-1}). (h) Schematic and SEM image of hierarchical gold clusters. The inset shows a magnified image of a single microparticle.

Experiments were conducted to determine whether the hierarchical gold cluster surface could be used as a waterproof electrode. Fig. 5a shows the image of the hierarchical gold cluster electrode fabricated on a flexible PDMS substrate. Parallel electrodes with 3 mm separation were deposited and electrical contact was made *via* the electrode pads on both ends. Negligible change in the water contact angle was observed after the substrate recovered from bending, indicating that the hierarchical gold cluster structure did not fracture after deformation (Fig. 5b). The applicability of the omniphobic gold electrodes was investigated by measuring the current–voltage (*I–V*) characteristics of the electrodes when a droplet of 0.12% PEDOT:PSS solution was placed on and between the electrodes (Fig. 5c).

Fig. 5d shows that the current was about 0.74 ± 0.11 μA at the applied voltage of 0.5 V for a PEDOT:PSS solution droplet deposited on the electrode without PFT treatment. However, once the electrode was subjected to hydrophobic treatment, the current was reduced by nearly five orders of magnitude (8.74 ± 3.21 pA) because of the very small contact area between the electrode and solution. Note that the current is affected not only by the resistance of the electrolyte but also by the actual contact area between the electrode and the electrolyte solution when an external voltage is applied. In addition, the water-sliding angle of the fabricated hierarchical gold cluster structure was very small (<5°), thus making it easy to remove water droplets from the electrode.

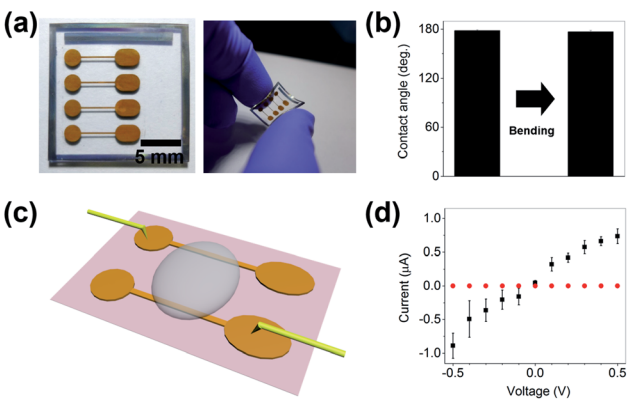

Fig. 5 (a) Photograph of hierarchical gold cluster-grown electrodes fabricated on a flexible PDMS substrate. (b) Change in the water contact angle of the omniphobic superhydrophobic electrode before and after bending. (c) Schematic of the experiment to evaluate the effect of a droplet of PEDOT:PSS solution on the conductivity. (d) The corresponding *I–V* characteristic curves of the electrodes with (red circles) and without (black squares) PFT treatment.

Conclusions

We fabricated a superomniphobic gold electrode by creating hierarchical gold clusters and nanoflakes on a gold electrode *via* a simple wet-chemical reduction reaction. Hierarchical gold clusters and gold nanoflakes were produced when the reduction reaction was repeated with a high hydroxylamine concentration whereas only gold nanoflakes were produced with a low hydroxylamine concentration. After the formation of a self-assembled monolayer of PFT on the hierarchical gold cluster-grown surface, the contact angles for both water and hexadecane were more than 150°. In addition, it was demonstrated that the hierarchical gold cluster structure could be patterned on a flexible substrate and act as liquid-repellent electrodes; the negative effect of water on the performance of the device was drastically reduced. The non-wetting and non-fouling properties of the omniphobic metal electrodes may be useful making wearable electronic sensing devices less vulnerable to sweat contamination.

Conflicts of interest

There are no conflicts to declare.

Acknowledgements

This work was supported by the Industrial Strategic Technology Development Program (10070241, Fabrication of High Bulk Porous Composite Sorbent with Pulp Support for Removal of Oil and Heavy Metals by Wet-laid Process) funded by the Ministry of Trade, Industry & Energy (MOTIE, Korea).

References

1 S. Pan, A. K. Kota, J. M. Mabry and A. Tuteja, *J. Am. Chem. Soc.*, 2012, **135**, 578–581.
2 S. Y. Lee, Y. Rahmawan and S. Yang, *ACS Appl. Mater. Interfaces*, 2015, **7**, 24197–24203.
3 X. Deng, L. Mammen, H.-J. Butt and D. Vollmer, *Science*, 2012, **335**, 67–70.

4 W. S. Wong, G. Liu, N. Nasiri, C. Hao, Z. Wang and A. Tricoli, *ACS Nano*, 2017, **11**, 587–596.
5 X. Yao, J. Gao, Y. Song and L. Jiang, *Adv. Funct. Mater.*, 2011, **21**, 4270–4276.
6 J. Lee, C. Boo, W.-H. Ryu, A. D. Taylor and M. Elimelech, *ACS Appl. Mater. Interfaces*, 2016, **8**, 11154–11161.
7 C. Boo, J. Lee and M. Elimelech, *Environ. Sci. Technol.*, 2016, **50**, 12275–12282.
8 W. Barthlott and C. Neinhuis, *Planta*, 1997, **202**, 1–8.
9 L. Feng, S. Li, Y. Li, H. Li, L. Zhang, J. Zhai, Y. Song, B. Liu, L. Jiang and D. Zhu, *Adv. Mater.*, 2002, **14**, 1857–1860.
10 X. Gao and L. Jiang, *Nature*, 2004, **432**, 36.
11 R. Hensel, C. Neinhuis and C. Werner, *Chem. Soc. Rev.*, 2016, **45**, 323–341.
12 X. Gao, L. P. Xu, Z. Xue, L. Feng, J. Peng, Y. Wen, S. Wang and X. Zhang, *Adv. Mater.*, 2014, **26**, 1771–1775.
13 J. Yang, Z. Zhang, X. Xu, X. Zhu, X. Men and X. Zhou, *J. Mater. Chem.*, 2012, **22**, 2834–2837.
14 A. K. Kota, G. Kwon, W. Choi, J. M. Mabry and A. Tuteja, *Nat. Commun.*, 2012, **3**, 1025.
15 L. Chen, Z. Guo and W. Liu, *J. Mater. Chem. A*, 2017, **5**, 14480–14507.
16 H. Zhao, K.-C. Park and K.-Y. Law, *Langmuir*, 2012, **28**, 14925–14934.
17 A. Tuteja, W. Choi, M. Ma, J. M. Mabry, S. A. Mazzella, G. C. Rutledge, G. H. McKinley and R. E. Cohen, *Science*, 2007, **318**, 1618–1622.
18 A. Ahuja, J. Taylor, V. Lifton, A. Sidorenko, T. Salamon, E. Lobaton, P. Kolodner and T. Krupenkin, *Langmuir*, 2008, **24**, 9–14.
19 T. Liu and C.-J. Kim, *Science*, 2014, **346**, 1096.
20 A. R. Bielinski, M. Boban, Y. He, E. Kazyak, D. H. Lee, C. Wang, A. Tuteja and N. P. Dasgupta, *ACS Nano*, 2016, **11**, 478–489.
21 K. Golovin, D. H. Lee, J. M. Mabry and A. Tuteja, *Angew. Chem., Int. Ed.*, 2013, **52**, 13007–13011.
22 A. K. Kota, Y. Li, J. M. Mabry and A. Tuteja, *Adv. Mater.*, 2012, **24**, 5838–5843.
23 K. N. Al-Milaji and H. Zhao, *Appl. Surf. Sci.*, 2017, **396**, 955–964.
24 J. Yang, Z. Zhang, X. Men, X. Xu and X. Zhu, *New J. Chem.*, 2011, **35**, 576–580.
25 P. S. Brown and B. Bhushan, *Philos. Trans. R. Soc., A*, 2016, **374**, 20160193.
26 C.-T. Hsieh, F.-L. Wu and W.-Y. Chen, *J. Phys. Chem. C*, 2009, **113**, 13683–13688.
27 Y. Liu, T. Ding, Q. Meng, B. Dong, L. Cao and R. Gao, *RSC Adv.*, 2016, **6**, 91669–91678.
28 L. Cao, T. P. Price, M. Weiss and D. Gao, *Langmuir*, 2008, **24**, 1640–1643.
29 Z. Xue, M. Liu and L. Jiang, *J. Polym. Sci., Part B: Polym. Phys.*, 2012, **50**, 1209–1224.
30 A. Steele, I. Bayer and E. Loth, *Nano Lett.*, 2008, **9**, 501–505.
31 R. Grynyov, E. Bormashenko, G. Whyman, Y. Bormashenko, A. Musin, R. Pogreb, A. Starostin, V. Valtsifer, V. Strelnikov and A. Schechter, *Langmuir*, 2016, **32**, 4134–4140.
32 G. Stremsdoerfer, H. Perrot, J. Martin and P. Clechet, *J. Electrochem. Soc.*, 1988, **135**, 2881–2886.
33 Z. Ma and S. F. Sui, *Angew. Chem., Int. Ed.*, 2002, **41**, 2176–2179.